Available online at www.sciencedirect.com

ScienceDirect

journal homepage: http://www.elsevier.com/locate/acme

Original Research Article

Analytical and experimental investigation on the free vibration of a floating composite sandwich plate having viscoelastic core

Seyed Saed Rezvani, Mehdi Saeed Kiasat *

Department of Maritime Engineering, Amirkabir University of Technology, Hafez Ave. 424, Tehran, Iran

ARTICLE INFO

Article history:
Received 11 December 2017
Accepted 29 March 2018
Available online 19 April 2018

Keywords:
Analytical vibration solution
Composite sandwich plate
Viscoelastic foam core
Modal testing

ABSTRACT

This paper focuses on the free vibration analytical solution of a composite sandwich plate consisting of woven carbon laminated faces and a viscoelastic foam core. In addition to the dry condition, a case of floating on bounded water is considered for the sandwich plate not only in analytical work but also in verification experiments. The equations of motion for the first-order shear-deformation plate in contact with the fluid are derived by using Hamilton's principle, and analytically solved using Navier's procedure. Bounded water boundary conditions and velocity potential function are used to describe the fluid motion. The viscoelastic properties of a marine PVC foam core are extracted from dynamic mechanical analysis. Frequency response function (FRF) method is applied in modal testing for measuring the natural frequencies of the dry and wet sandwich plates. Experimental results demonstrate the validity of the analytical results. The effects of the foam core behavior, core thickness, plate dimension ratio, and the fluid density on the natural frequencies are examined and discussed. The decrease of the fundamental mode natural frequency with the presence of the viscoelastic foam core is more prominent for the dry sandwich plate with respect to the wet one already damped by water.

1. Introduction

Lightweight composite sandwich panels are widely used as the main load-carrying body of aerospace, civil, and marine vessels. Composite sandwich plates consisting of two thin stiff composite faces and a thicker flexible core layer show proper behavior under bending due to an increased flexural stiffness. In addition, significant viscoelastic behavior of sandwich plates helps the damping of vibration and noise. The viscoelastic behavior of the sandwich plates is mainly due to their flexible core material. Several different materials used for sandwich core in marine applications like PVC foams are known to be viscoelastic materials having time- and frequency-dependent properties. The viscoelastic behavior of the core material decreases the natural frequencies of the sandwich plate in free vibration. On the other hand, the composite

* *Corresponding author.*
E-mail address: kiasat@aut.ac.ir (M.S. Kiasat).

https://doi.org/10.1016/j.acme.2018.03.006

sandwich body of a marine structure may have different natural frequencies in and out of water, known as dry and wet natural frequencies. The decrease of the natural frequencies is attributed to the effect of the added mass of water.

The free vibration of composite sandwich plates has been studied in the previous works. Cupial and Niziol [1] numerically calculated the natural frequencies and loss factors for a plate assuming simplified viscoelastic properties for the core layer only in a dry condition. Kant and Swaminathan [2] derived an analytical solution to the natural frequency analysis of simply supported dry sandwich plates considering only elastic behavior for the face and core materials. A discrete layer annular finite element was employed to derive the equations of motion for a three-layered annular dry sandwich plate with a viscoelastic core layer by Wang and Chen [3]. Kim [4] examined the dynamic behavior of dry composite laminate plates undergoing moderately large deflection by considering the viscoelastic properties of the material. Xu et al. [5] presented a simplex optimization analysis method of dry metal structures with simple viscoelastic dampers. Chen [6] analyzed the non-axisymmetric vibration and stability problem of the rotating dry sandwich plate with a simple viscoelastic core layer by using the finite element method. Civalek [7] developed a discrete singular convolution method for the vibration analysis of moderately thick symmetrically dry composite laminate plates based on the first-order shear deformation theory.

The first-order shear deformation theory (FSDT) has been found to yield accurate results in the non-local problems of sandwich structures, such as buckling and free vibration [8]. A comparison between higher-order and first-order shear deformation theories for analyzing dry laminated composite stiffened plates was presented by Bhar et al. [9] using the finite element method. They clearly showed that the higher-order shear deformation theory tenders very close results with first-order shear deformation theory for un-stiffened even thick laminated composites. However, Bhar et al. [9] found significant differences between these two theories for stiffened composite laminates which was attributed to the realistic variation of transverse shear through the thickness due to the presence of the stiffeners. Several works have reasonably used the first-order shear deformation theory for polymeric laminated composites as well as functionally graded shells enhanced with composites, not only as flat plates [10] but also as annular ones [11].

Dynamic response of orthotropic viscoelastic laminated composite plates was investigated by Assie et al. [12] using an efficient numerical algorithm in time domain. Mahmoudkhani et al. [13] studied the free vibration and transverse response of dry sandwich plates with viscoelastic cores under wide-band random excitations. Kramer et al. [14] investigated the effects of material anisotropy and added mass on the free vibration response of elastic cantilevered composite laminate plates via combined analytical and numerical modeling. Yang et al. [15] experimentally investigated vibration and damping performances of composite pyramidal truss sandwich panels with viscoelastic layers embedded in the face layers. Khorshid and Farhadi [16] analyzed the vibration of an elastic composite laminate plate in contact with a bounded fluid.

Due to the lack of the analytical solution, the effect of the compressible flow on composite as well as functionally graded plates has been numerically examined [17]. The free vibration of isotropic viscoelastic plates on viscoelastic medium was analytically investigated by Kiasat et al. [18]. Avcar [19] examined separate and combined effects of rotary inertia, shear deformation and material non-homogeneity (MNH) on the values of natural frequencies of the simply supported beam. Yang et al. [20] provided a unified yet accurate solution for vibration and damping analysis of simple viscoelastic and functionally graded dry sandwich plates with arbitrary boundary conditions. Finally, Kahya and Turan [21] presented a finite element model based on the first-order shear deformation theory for free vibration and buckling of functionally graded beams.

In the present work, a composite sandwich plate consisting of woven carbon laminated faces and a low density PVC foam core is subjected to an experimental modal analysis. The measurements are done on a free-free square sandwich plate in both dry and wet conditions so that only one side of the plate is in contact with water. Frequency response function (FRF) method is applied to extract the natural frequencies of the sandwich plate. On the other hand, the equations of motion for the first-order shear-deformation plate coupled with the irrotational bounded water are analytically solved using Navier's solution to obtain the natural frequencies. The viscoelastic properties of the PVC foam core including master curves for the relaxation moduli are experimentally extracted using dynamic mechanical analysis as in our recent work on compound materials [22]. The analytical solution of the equations of motion introduces direct relations between the natural frequencies and the mechanical and physical properties of the sandwich and water, applicable in the modern sandwich marine vessels. Experimental results demonstrate the validity of the analytical results. The effects of the core viscoelastic properties and thickness, plate dimension ratio, and fluid density on the natural frequency are examined and discussed.

2. Equations of motion and analytical solution

The governing equations for the free vibration of a thick sandwich plate are derived using the first-order shear-deformation plate theory. The ratio of the thickness to the side length of sandwich plates is usually more than 1–15, and thus the shear deformation during bending causes a significant deviation from simple plate theory. On the other hand, no discontinuity is assumed to exist at the interfaces between the core and the laminate face layers. For small-amplitude vibration of symmetric sandwich plates considered in the present work, no interface failure or delamination, and no deviation of the neutral plane is expected. Furthermore, the core material is regarded to be viscoelastic having frequency-dependent storage and loss moduli which results in a significant damping behavior of the sandwich plate. Because of the presence of stiff fibers in the composite laminates, the faces show negligible viscoelastic behavior, and thus the laminates are assumed to be elastic.

2.1. Displacement field in thick plates

Based on the first-order shear-deformation theory, the displacement components u, v and w in x, y and z directions, respectively, in a thick vibrating plate of Fig. 1 are functions of the coordinates and time t as in Eq. (1). The origin of the orthonormal coordinate system (x, y, z) is chosen at the mid-surface of the sandwich plate.

$$\left.\begin{aligned} u(x,y,z,t) &= u_0(x,y,t) + z\theta_x(x,y,t) \\ v(x,y,z,t) &= v_0(x,y,t) + z\theta_y(x,y,t) \\ w(x,y,t) &= w_0(x,y,t) \end{aligned}\right\} \tag{1}$$

The functions θ_x and θ_y are rotations of the normal to the middle plane about y and x axes, respectively. Also u_0, v_0, w_0, θ_x and θ_y are defined at the reference plane, $z = 0$. By substituting Eq. (1) into the strain–displacement kinematic relations, the strain components are obtained as in Eq. (2).

$$\begin{aligned} \epsilon_{xx} = \epsilon_1 = \epsilon_{x0} + zk_x \quad &, \quad \epsilon_{yz} = \epsilon_4 = \frac{\partial w_0}{\partial y} + \theta_y = \varphi_y \\ \epsilon_{yy} = \epsilon_2 = \epsilon_{y0} + zk_y \quad &, \quad \epsilon_{xz} = \epsilon_5 = \frac{\partial w_0}{\partial x} + \theta_x = \varphi_x \\ \sigma_z = \sigma_3 = 0 \quad &, \quad \epsilon_{xy} = \epsilon_6 = \epsilon_{xy_0} + zk_{xy} \end{aligned} \tag{2}$$

where

$$\begin{aligned} (\epsilon_{x0}, \epsilon_{y0}, \epsilon_{xy0}) &= \left(\frac{\partial u_0}{\partial x}, \frac{\partial v_0}{\partial x}, \frac{\partial u_0}{\partial y} + \frac{\partial v_0}{\partial x}\right) \\ (k_x, k_y, k_{xy}) &= \left(\frac{\partial \theta_x}{\partial x}, \frac{\partial \theta_y}{\partial y}, \frac{\partial \theta_x}{\partial y} + \frac{\partial \theta_y}{\partial x}\right) \end{aligned} \tag{3}$$

2.2. Constitutive equations for laminated plates

The reduced stress tensor in any unidirectional ply of the upper and lower laminate faces, in the ply principal coordinates, are expressed as

$$\begin{aligned} \{\sigma\}^{(k)} = [Q]^{(k)}\{\epsilon\}^{(k)}, \quad &\begin{Bmatrix} \sigma_1 \\ \sigma_2 \\ \sigma_4 \\ \sigma_5 \\ \sigma_6 \end{Bmatrix}^{(k)} \\ = &\begin{bmatrix} Q_{11} & Q_{12} & 0 & 0 & 0 \\ Q_{21} & Q_{22} & 0 & 0 & 0 \\ 0 & 0 & G_{23} & 0 & 0 \\ 0 & 0 & 0 & G_{13} & 0 \\ 0 & 0 & 0 & 0 & G_{12} \end{bmatrix}^{(k)} \begin{Bmatrix} \epsilon_1 \\ \epsilon_2 \\ \epsilon_4 \\ \epsilon_5 \\ \epsilon_6 \end{Bmatrix} \end{aligned} \tag{4}$$

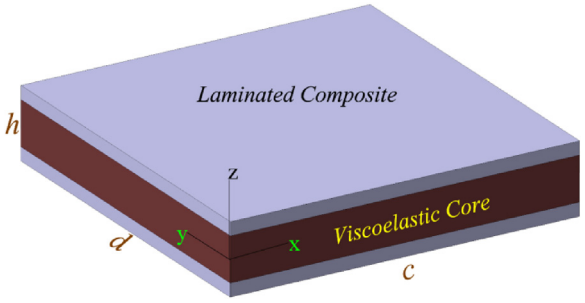

Fig. 1 – The coordinate system for the sandwich plate.

The superscript (k) refers to the kth ply within the laminate. The terms Q_{ij} and G_{ij} represent the stiffness constants for a unidirectional orthotropic ply in its principal coordinates. Eq. (4) is transformed to the sandwich plate coordinates (x, y, z) in which the strain components (2) are substituted to obtain

$$\begin{aligned} \{\sigma'\}^{(k)} = [Q']^{(k)}\{\epsilon'\}^{(k)}, \quad &\begin{Bmatrix} \sigma_1 \\ \sigma_2 \\ \sigma_4 \\ \sigma_5 \\ \sigma_6 \end{Bmatrix}^{(k)} \\ = [Q']^{(k)} &\begin{Bmatrix} \epsilon_{x0} \\ \epsilon_{y_0} \\ \varphi_y \\ \varphi_x \\ \epsilon_{xy_0} \end{Bmatrix} + z[Q']^{(k)} \begin{Bmatrix} k_x \\ k_y \\ 0 \\ 0 \\ k_{xy} \end{Bmatrix}, \quad z_{k-1} < z < z_k \end{aligned} \tag{5}$$

where $[Q']^{(k)}$ is the 5×5 stiffness matrix of the kth layer transformed into the plate coordinates. The distributed force and moment resultants applied on the laminate side lengths are obtained by integrating the stresses over the thickness of the laminate as below

$$\begin{aligned} \{N\} = \begin{Bmatrix} N_x \\ N_y \\ Q_y \\ Q_x \\ N_{xy} \end{Bmatrix} &= \left[\sum_{k=1}^{n} \int_{z_{k-1}}^{z_k} \begin{Bmatrix} \sigma_1 \\ \sigma_2 \\ \sigma_4 \\ \sigma_5 \\ \sigma_6 \end{Bmatrix} dz\right] \\ = [A] &\begin{Bmatrix} \epsilon_{x_0} \\ \epsilon_{y_0} \\ \varphi_y \\ \varphi_x \\ \epsilon_{xy} \end{Bmatrix} + [B] \begin{Bmatrix} k_x \\ k_y \\ 0 \\ 0 \\ k_{xy} \end{Bmatrix} \end{aligned} \tag{6}$$

$$\begin{aligned} \{M\} = \begin{Bmatrix} M_x \\ M_y \\ M_{yz} \\ M_{xz} \\ M_{xy} \end{Bmatrix} &= \left[\sum_{k=1}^{n} \int_{z_{k-1}}^{z_k} z \begin{Bmatrix} \sigma_1 \\ \sigma_2 \\ \sigma_4 \\ \sigma_5 \\ \sigma_6 \end{Bmatrix} dz\right] \\ = [B] &\begin{Bmatrix} \epsilon_{x_0} \\ \epsilon_{y_0} \\ \varphi_y \\ \varphi_x \\ \epsilon_{xy} \end{Bmatrix} + [D] \begin{Bmatrix} k_x \\ k_y \\ 0 \\ 0 \\ k_{xy} \end{Bmatrix} \end{aligned} \tag{7}$$

The matrices [A], [B] and [D] are the composite laminate stiffness matrices defined as follows

$$\begin{aligned} \{A_{ij} \quad B_{ij} \quad D_{ij}\} = \sum_{k=1}^{n} \int_{z_{k-1}}^{z_k} Q_{ij}^{\prime(k)} \{1 \quad z \quad z^2\} dz \quad (i,j \\ = 1,2,3,4,5), \end{aligned} \tag{8}$$

where the distance $z_k - z_{k-1}$ is the thickness of a single ply of the laminate faces.

2.3. Constitutive equations for the viscoelastic foam

A viscoelastic material is characterized by its creep or relaxation behavior under a constant-load or a constant-deformation excitation, respectively. Under a harmonic excitation, the viscoelastic material is described by its storage

and loss moduli. On the other hand, the viscoelastic behavior presents itself by material damping in a free vibration excitation. Within the limits of linear viscoelasticity, the Boltzmann superposition principle is used to derive the stress–strain constitutive relation based on the relaxation functions, $C_{ij}(t)$, of the material

$$\sigma_i(t) = \int_{-\infty}^{t} C_{ij}(t-\tau)\frac{d\epsilon_j(\tau)}{d\tau}d\tau \tag{9}$$

where $\varepsilon_j(\tau) = 0$ for $-\infty < \tau < 0$ and the components of the relaxation function matrix C_{ij} are combinations of the Young's and shear relaxation moduli. In a damped free vibration the harmonic strain applied to the viscoelastic material may be described by an exponential function of time with a complex frequency as below:

$$\epsilon_j(t) = \epsilon_{0j}e^{\omega^* t}, \quad \omega^* = (-\beta\omega + i\omega) \tag{10}$$

where ε_{0j}, ω^*, ω and β are the initial amplitude, complex frequency, natural frequency and damping factor, respectively. The negative real part of the complex frequency introduces the decreasing amplitude of the damped vibration. By substituting Eq. (10) into Eq. (9) and using $\eta = t - \tau$, the stress is obtained as

$$\sigma_i(t) = \int_0^{\infty} C_{ij}(\eta)(-\beta\omega + i\omega)\epsilon_{0j}e^{(-\beta\omega+i\omega)(t-\eta)}d\eta \tag{11}$$

By applying harmonic functions for $e^{-(-\beta\omega+i\omega)\eta}$ in the integration, and extracting $e^{(-\beta\omega+i\omega)t}$ from the integration on η, the above equation changes to

$$\sigma_i(t) = \left[\int_0^{\infty} \omega C_{ij}(\eta)e^{\beta\omega\eta}(\sin(\omega\eta) - \beta\cos(\omega\eta))d\eta\right.$$
$$\left. + i\int_0^{\infty} \omega C_{ij}(\eta)e^{\beta\omega\eta}(\cos(\omega\eta) + \beta\sin(\omega\eta))d\eta\right]\epsilon_{0j}e^{(-\beta\omega+i\omega)t} \tag{12}$$

Since the effect of the harmonic terms containing the small damping factor, β, is negligible in the integrations, the integrals in Eq. (12) may be reduced to the following form:

$$\sigma_i(t) = \left[\underbrace{\int_0^{\infty} \omega C_{ij}(\eta)\sin(\omega\eta)d\eta}_{C'_{ij}(\omega)} + i\underbrace{\int_0^{\infty} \omega C_{ij}(\eta)\cos(\omega\eta)d\eta}_{C''_{ij}(\omega)}\right]\epsilon_j(t) \tag{13}$$

The two integrals in the bracket of Eq. (13) are known as the storage and loss moduli, $C'_{ij}(\omega)$ and $C''_{ij}(\omega)$ respectively, which are functions of the frequency. The combination of these two moduli indicates the complex modulus of the viscoelastic material as shown below:

$$C^*_{ij}(\omega) = C'_{ij}(\omega) + iC''_{ij}(\omega) \text{ and then } \sigma_i(t) = C^*_{ij}(\omega)\epsilon_j(t) \tag{14}$$

In expanded matrix notation, all nonzero components of stress in Eq. (14) are written as:

$$\begin{Bmatrix}\sigma_1(t)\\ \sigma_2(t)\\ \sigma_4(t)\\ \sigma_5(t)\\ \sigma_6(t)\end{Bmatrix} = \begin{bmatrix} C^*_{11}(\omega) & C^*_{12}(\omega) & 0 & 0 & 0\\ C^*_{21}(\omega) & C^*_{22}(\omega) & 0 & 0 & 0\\ 0 & 0 & C^*_{44}(\omega) & 0 & 0\\ 0 & 0 & 0 & C^*_{55}(\omega) & 0\\ 0 & 0 & 0 & 0 & C^*_{66}(\omega)\end{bmatrix} \times \begin{Bmatrix}\epsilon_1(t)\\ \epsilon_2(t)\\ \epsilon_4(t)\\ \epsilon_5(t)\\ \epsilon_6(t)\end{Bmatrix} \tag{15}$$

The stress–strain relation for the viscoelastic core material in Eq. (15) is applied as a single layer in the Eqs. (6) and (7) to form the complete load-deformation relations for the sandwich plate.

2.4. *Hydrodynamic model*

The fluid is assumed to be homogeneous, incompressible, inviscid, irrotational, and its motion is small, because of the small amplitude of the plate vibrations. Therefore, the velocity potential $\phi(x, y, z, t)$ must satisfy Laplace's equation given by [23]:

$$\nabla^2\phi = \frac{\partial^2\phi}{\partial x^2} + \frac{\partial\phi}{\partial y^2} + \frac{\partial^2\phi}{\partial z^2} = 0 \tag{16}$$

The boundary conditions at the fluid/tank rigid wall interfaces are given as zero velocities,

$$\begin{cases}\dfrac{\partial\phi}{\partial x} = 0 & \text{on} \quad x = 0, c\\ \dfrac{\partial\phi}{\partial y} = 0 & \text{on} \quad y = 0, d\\ \dfrac{\partial\phi}{\partial z} = 0 & \text{on} \quad z = a\end{cases} \tag{17}$$

The boundary condition at the fluid/sandwich plate interface is expressed as equal velocities for the fluid and the vibrating plate,

$$\frac{\partial\phi}{\partial z}\Big|_{Z=0} = \frac{\partial W(x, y, t)}{\partial t} \tag{18}$$

In order to solve the Laplace's differential equation, a separation of variable form is assumed for the velocity potential function,

$$\phi(x, y, z, t) = G(x, y, t)F(z) \tag{19}$$

where $F(z)$ and $G(x,y,t)$ are two functions to be determined. By substituting Eq. (19) into the boundary condition (18), we arrive at the following equation

$$G(x, y, t) = \frac{1}{\frac{dF}{dz}|_{z=0}}\frac{\partial W}{\partial t} \tag{20}$$

Eq. (20) describes the movement of the fluid at any point on the interface linked to the movement of the plate. After substituting Eq. (20) into Eq. (19), the following expression for the potential function is derived

$$\phi(x,y,z,t)=\frac{F(z)}{\frac{dF}{dz}|_{z=0}}\frac{\partial W}{\partial t} \tag{21}$$

Substituting Eq. (21) into Laplace's equation described in the Eq. (16) leads to the following differential equation

$$\frac{d^2F(z)}{dz^2}-\mu^2F(z)=0 \tag{22}$$

The general solution of Eq. (22) is given as

$$F(z)=C_1e^{\mu z}+C_2e^{-\mu z} \tag{23}$$

where C_1 and C_2 are two unknown integration constants and μ is determined after solving the differential equation of the velocity potential function using the boundary conditions in x and y directions. The general solution of $G(x, y, t)$ is given as

$$G(x,y,t)=C\ \cos(\lambda x)\ \cos((\mu^2-\lambda^2)y)T(t) \tag{24}$$

where $\lambda=\frac{\pi}{c}$, $\mu=\pi\sqrt{\frac{1}{c^2}+\frac{1}{d^2}}$ and C is constant.

Applying boundary conditions (17) and (18) into Eq. (23) and using Eq. (21), the potential function can be derived as follows

$$\phi(x,y,z,t)=\frac{1}{\mu}\left[\frac{e^{\mu(z-2a)}+e^{-\mu z}}{e^{-2\mu a}-1}\right]\frac{\partial W}{\partial t} \tag{25}$$

The kinetic energy of the fluid with a density of ρ_w is expressed using the above velocity potential function

$$T_w=\frac{1}{2}\rho_w\int_{\Omega}(\nabla\varphi)^2d\Omega \tag{26}$$

By applying Green's theorem, the volume integral on the fluid domain Ω, is transformed into a surface integral over the plate surface Γ as follows

$$T_w=-\frac{1}{2}\rho_w\int_{\Gamma}\left(\varphi\frac{\partial\varphi}{\partial z})|_{z=0}\right)d\Gamma \tag{27}$$

2.5. *Hamilton's principle*

Hamilton's principle for free vibration analysis of a wet plate can be written as follows:

$$\delta\int_0^t[T+T_w-U]dt=0 \tag{28}$$

where U and T are the potential strain energy and kinetic energy of the plate respectively, and T_w the fluid kinetic energy as in Eq. (27). Substituting energy expressions into the Hamilton's principle, the following relation is obtained

$$0=\int_0^t\Big[-\int_{-h/2}^{h/2}\int_A(\sigma_x\delta\epsilon_x+\sigma_y\delta\epsilon_y+\sigma_{xy}\delta\epsilon_{xy}+\kappa\sigma_{yz}\delta\epsilon_{yz}+\kappa\sigma_{xz}\delta\epsilon_{xz})dAdz+\frac{1}{2}\int_{-h/2}^{h/2}\int_A\rho\delta\left[(\dot{u}_w)^2+(\dot{v}_w)^2+(\dot{w}_w)^2\right]dAdz+\delta T_w\Big]dt \tag{29}$$

where ρ is the density for each layer, and κ the shear correction factor. The shear correction factor is introduced in the first-order shear-deformation theory to compensate the effect of the assumption of uniform shear strain over the thickness. An approximate value of 5/6 ≈0.833 for the shear correction factor has been common in the literature for plates. However, Birman and Bert [8] showed that the value of the shear correction factor may differ for homogeneous plates and sandwich structures. Two values of $\pi^2/12\approx0.822$ and $5/(6-\nu)\approx0.877$ are proposed in Mindlin plate theory for homogeneous and sandwich plates, respectively. Also it has been shown that the shear correction factor for sandwich plates is affected by both thicknesses as well as the stiffnesses of the facings and core materials. Pradeep et al. [24] presented the effects of these parameters in two graphs which give the value of the shear correction factor between 0.833 and 0.88. Taking all the above points into account, a reasonable value of $\sqrt{3}/2\approx0.866$ [16] is used in the present work for our symmetric sandwich plate specified in the next sections.

It is noted that because of the symmetry of the sandwich plate considered in our work, the deviation of the neutral plane is not expected specially for the small amplitude vibration. Using Eqs. (1)–(3), (27) into (29) and integrating the resulting expression by part, and separating the coefficients of δu_0, δv_0, δw_0, θ_x and θ_y, the following differential equations of motion are obtained:

$$\begin{aligned}
&\delta u_0: \frac{\partial N_x}{\partial x}+\frac{\partial N_{xy}}{\partial y}=I_1\ddot{u}_0+I_2\ddot{\theta}_x\\
&\delta v_0: \frac{\partial N_y}{\partial y}+\frac{\partial N_{xy}}{\partial x}=I_1\ddot{v}_0+I_2\ddot{\theta}_y\\
&\delta w_0: \frac{\partial Q_x}{\partial x}+\frac{\partial Q_y}{\partial y}=\ddot{w}_0(I_1+m_a)\\
&\delta\theta_x: \frac{\partial M_x}{\partial x}+\frac{\partial M_{xy}}{\partial y}+\kappa Q_x=I_2\ddot{u}_0+I_3\ddot{\theta}_x\\
&\delta\theta_y: \frac{\partial M_y}{\partial y}+\frac{\partial M_{xy}}{\partial x}+\kappa Q_y=I_2\ddot{v}_0+I_3\ddot{\theta}_y
\end{aligned} \tag{30}$$

where m_a is the added mass obtained using the following relation [25]

$$m_a=\rho_w\frac{1}{2\mu^2}\frac{(e^{-2a\mu}+1)}{(e^{-2a\mu}-1)}(\mu\,e^{(-2a\mu)}-\mu) \tag{31}$$

$$I_1,I_2,I_3=\int_{-h/2}^{h/2}\rho(1,z,z^2)dz \tag{32}$$

By inserting Eqs. (5) and (15) into Eqs. (6) and (7), and integrating through the thickness of the sandwich plate, the force and moment resultants are obtained (see Appendix A). The force and moment resultants are substituted in Eq. (30) to achieve five differential equations of motion (see Appendix B).

2.6. Analytical solutions

In the present work, the differential equations of motion are analytically solved for a $c \times d$ rectangular sandwich plate by using the Navier's solution procedure [26] for displacement components u, v, w and rotations θ_x and θ_y.

$$\begin{aligned} u_0(x,y,t) &= \sum_{m=1}^{M}\sum_{n=1}^{N} u_{m,n}\cos(\alpha x)\sin(\beta y)e^{-i\omega t} \\ v_0(x,y,t) &= \sum_{m=1}^{M}\sum_{n=1}^{N} v_{m,n}\sin(\alpha x)\cos(\beta y)e^{-i\omega t} \\ w_0(x,y,t) &= \sum_{m=1}^{M}\sum_{n=1}^{N} w_{m,n}\sin(\alpha x)\sin(\beta y)e^{-i\omega t} \\ \theta_x(x,y,t) &= \sum_{m=1}^{M}\sum_{n=1}^{N} \theta_{x\,m,n}\cos(\alpha x)\sin(\beta y)e^{-i\omega t} \\ \theta_y(x,y,t) &= \sum_{m=1}^{M}\sum_{n=1}^{N} \theta_{y\,m,n}\sin(\alpha x)\cos(\beta y)e^{-i\omega t} \end{aligned} \tag{33}$$

where $\alpha = \frac{m\pi}{c}$ and $\beta = \frac{n\pi}{d}$, are the unknown coefficients. $u_{m,n}$, $v_{m,n}$, $w_{m,n}$, $\theta_{x\,m,n}$, $\theta_{y\ m,n}$ are to be determined. The above displacement components are proposed for a plate having four simply supported sides described by the following boundary conditions

$$\begin{aligned} u = v = w = \theta_y = M_x = 0 \quad \text{at} \quad x = 0,\ c \\ u = v = w = \theta_x = M_y = 0 \quad \text{at} \quad y = 0,\ d \end{aligned} \tag{34}$$

When the solution form for the displacement components (33) are substituted into the differential equations of motion resulted from (30), a set of homogeneous algebraic equations are obtained which can be written in matrix form as follows

$$([K^*(\omega)] - \lambda^*[M])\{U^*\} = \{0\} \tag{35}$$

where $\lambda^* = (\omega^*)^2$ and $\{U^*\}$ are the complex eigenvalues and the eigenvectors, respectively. The complex stiffness matrix $[K^*(\omega)]$ is composted of the real and imaginary parts $[K^*(\omega)] = [K'(\omega)] + i\,[K''(\omega)]$ due to the dynamic modulus of the viscoelastic foam in (13). After solving Eq. (35), the complex eigenvalues are obtained as $\lambda^* = \lambda' + i\lambda''$. The natural frequency ω of the sandwich plate can be calculated as follows:

$$\left\{ \begin{bmatrix} k'_{11} & k'_{12} & k'_{13} & k'_{14} & k'_{15} \\ k'_{21} & k'_{22} & k'_{23} & k'_{24} & k'_{25} \\ k'_{31} & k'_{32} & k'_{33} & k'_{34} & k'_{35} \\ k'_{41} & k'_{42} & k'_{43} & k'_{44} & k'_{45} \\ k'_{51} & k'_{52} & k'_{53} & k'_{54} & k'_{55} \end{bmatrix} - \lambda' \begin{bmatrix} m_{11} & m_{12} & m_{13} & m_{14} & m_{15} \\ m_{21} & m_{22} & m_{23} & m_{24} & m_{25} \\ m_{31} & m_{32} & m_{33} & m_{34} & m_{35} \\ m_{41} & m_{42} & m_{43} & m_{44} & m_{45} \\ m_{51} & m_{52} & m_{53} & m_{54} & m_{55} \end{bmatrix} \right\} \begin{Bmatrix} u_{m,n} \\ v_{m,n} \\ w_{m,n} \\ \theta_{xm,n} \\ \theta_{ym,n} \end{Bmatrix} = \begin{Bmatrix} 0 \\ 0 \\ 0 \\ 0 \\ 0 \end{Bmatrix} \tag{36}$$

where $[K']$, $[M]$ and $\omega = \sqrt{\lambda'}$ are the real part of the stiffness matrix, the mass matrix and the natural frequency of the sandwich plate in contact with a bounded fluid, respectively. The elements of the stiffness and mass matrices are presented in Appendix C.

3. Materials specification and properties

In the experimental part of this work, a sandwich panel is fabricated using eight layers of a thick woven carbon fabric and a layer of PVC foam. All layers together are impregnated by an epoxy resin through the vacuum infusion process. The nominal thickness of the sandwich panel is 20 mm consisting of two 2.5 mm thick face laminates and 15 mm thick PVC foam core. A square sandwich plate of 270 mm side length is cut out of the vacuumed panel. The specifications of the fabric and foam and their mechanical properties required for the analytical calculations are detailed in the following sections. The isotropic viscoelastic properties of the foam core C_{ij} in Eq. (9) are collected from dynamic mechanical analysis (DMA) using both extension and shear deformations. On the other hand, the orthotropic elastic properties of the face laminates [Q] in Eq. (4) are extracted from our relevant work [27] as explained in the following sections.

3.1. Foam viscoelastic properties

The foam core selected for the present work is AIREX-C70.75 a closed cell PVC foam with a density of 75 kg/m^3. In order to obtain the long term viscoelastic properties of the foam core over more than 13 frequency decades, the dynamic tests are performed in a wide range of the constant temperatures. For a viscoelastic material as foam, the rate of the relaxation or creep behavior increases with the temperature. Based on the time-temperature superposition principle, the effect of the temperature is treated as a reduced time, and on this basis a master curve is developed for the viscoelastic properties [22,28].

In this work, both compressive and shear deformation DMA tests are performed at 7 different constant temperatures −25, −10, 0, 10, 25, 35, 50 °C in a DMA machine equipped with a cooling/heating chamber shown in Fig. 2. The configurations of the foam specimen for the compressive and shear DMA test are presented in Fig. 3. At each temperature a sweep of frequency of 0.01, 0.02, 0.05, 0.1, 0.2, 0.5, 1, 2, 5, 10, 20, 50,100 Hz is carried out, and the storage Young's and shear Moduli are obtained as functions of temperature and frequency, shown in Figs. 4 and 5, respectively.

Based on the time-temperature superposition principle, the effect of the increase or decrease of the temperature is treated as the decrease or increase of frequency, respectively. According to this analogy, the measured values of the storage modulus at different temperatures over a limited frequency range are taken as the short-term parts of a single long-term master curve over a wide frequency range. On this basis, to construct the master curve for the storage modulus, the curve at 25 °C in Figs. 4 and 5 is selected as the modulus at the reference temperature. The other curves at the higher and lower temperatures are then shifted horizontally to the left and right, respectively, over the logarithmic frequency axis to meet the other curves. The shifting process is performed by multiplying the frequency axis by an appropriate shift factor $a(T)$ at each temperature. Figs. 6 and 7 present the master curves developed in this work for the storage Young's and shear moduli of the PVC foam, respectively, over more than 13

Fig. 2 – The DMA test setups.

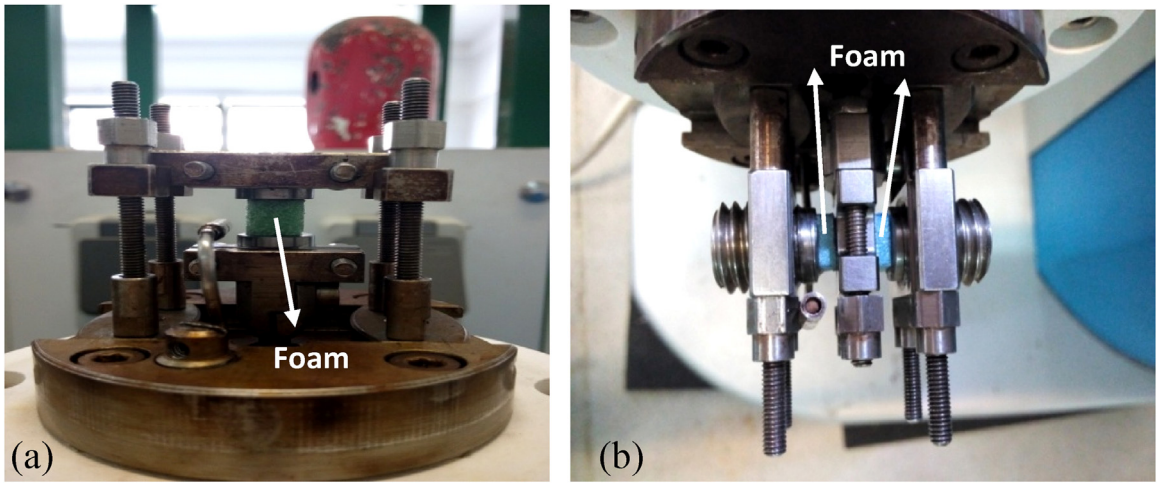

Fig. 3 – PVC foam core subjected to (a) compression excitation and (b) shear excitation.

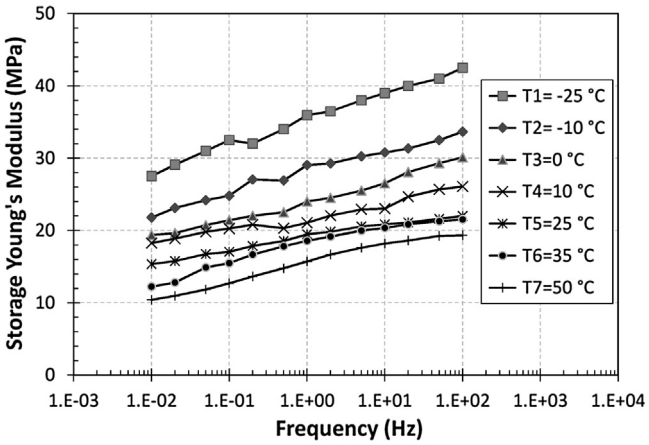

Fig. 4 – Storage Young's modulus at seven temperatures.

frequency decades. Also the data obtained for the shift factor of the foam for the construction of the master curve is shown in Fig. 8.

When the decreasing behavior of the relaxation modulus in time domain described by a Prony exponential series is substituted in the viscoelastic constitutive relation (9), the increasing behavior of the storage modulus in frequency domain is obtained as a fractional series. On this basis, the fractional series (37) and (38) are fitted to the master curves data for the storage Young's and shear moduli in Figs. 6 and 7, respectively. The constant intensities E_i and G_i, and the relaxation times τ_i for the PVC foam are obtained from the fitting process over 13 frequency decades and presented in Table 1.

$$E(t) = \sum_{i=1}^{n} E_i \exp\left(\frac{-t}{\tau_i}\right) \Rightarrow E'(\omega) = \sum_{i=1}^{n} E_i \frac{\omega^2 \tau_i^2}{1+\omega^2 \tau_i^2} \tag{37}$$

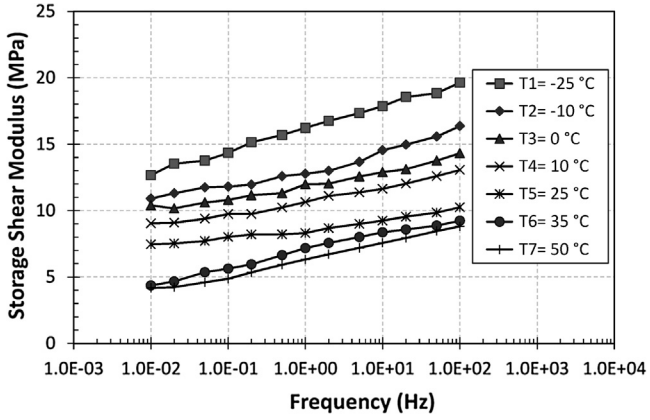

Fig. 5 – Storage shear modulus in various temperature.

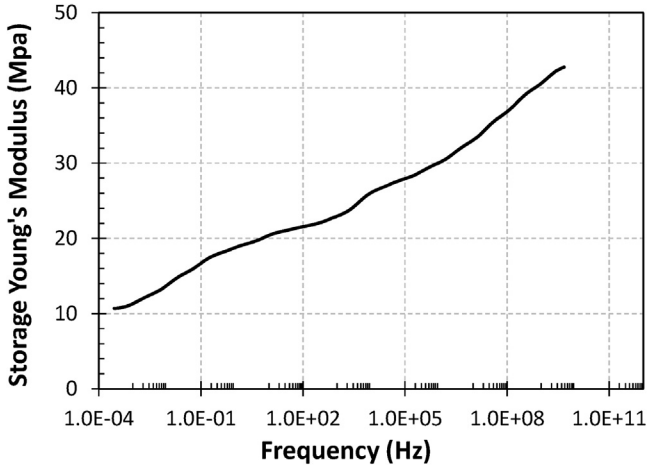

Fig. 6 – Master curve of the storage Young's modulus at reference temperature 25 °C.

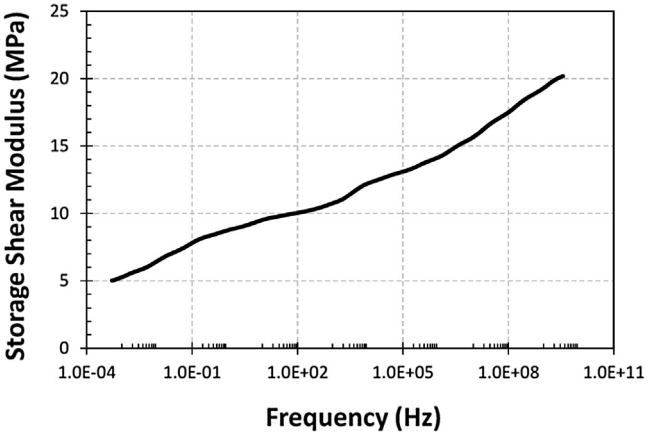

Fig. 7 – Master curve of the storage shear modulus at reference temperature 25 °C.

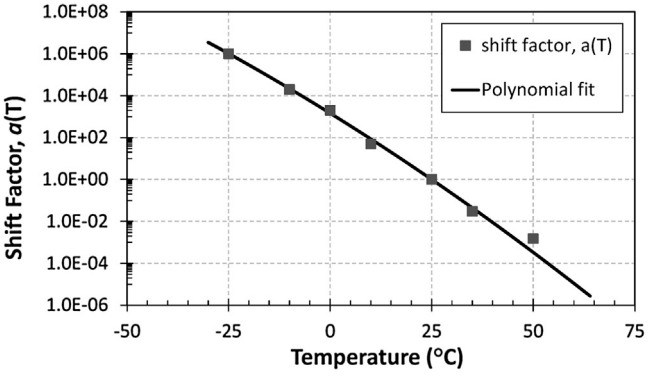

Fig. 8 – The shift factor *a*(T) and polynomial fitting.

$$G(t) = \sum_{i=1}^{n} G_i \exp\left(\frac{-t}{\tau_i}\right) \Rightarrow G'(\omega) = \sum_{i=1}^{n} G_i \frac{\omega^2 \tau_i^2}{1+\omega^2 \tau_i^2} \tag{38}$$

Among the mathematical models proposed in the literature for describing the variation of the shift factor versus temperature, a second-degree polynomial function proposed by Kiasat et al. [29] in Eq. (39) is best fitted to the shift factor data for the foam in Fig. 8.

$$\log(a) = c_1(T - T_{ref}) + c_2(T - T_{ref})^2 \tag{39}$$

where T_{ref} is the reference temperature (25 °C) and the constants c_1 and c_2 are obtained in the fitting process as -0.1328 and -2.54×10^{-4}, respectively. The above viscoelastic properties for the foam core of the sandwich plate are combined to obtain the components of the relaxation function matrix $C_{ij}(t)$.

3.2. *Face laminate properties*

The face laminates of the sandwich plate consist of 4 woven carbon/epoxy layers. The 12K-roving carbon fabric has an areal density and thickness of 600 g/m^2 and 0.6 mm, respectively [27]. Because of the complexity of the woven fabric composites as a single bidirectional layer, each of the woven carbon/epoxy layers is here modeled as a symmetric 4-ply laminate [90/0/0/90] as done in [30]. The properties of such a laminate are obtained from the orthotropic elastic properties of its constituting unidirectional plies measured as presented in Table 2.

4. Experimental modal analysis

In order to prepare a free-free boundary condition for the sandwich plate undergoing modal analysis, shown in Fig. 9, the plate is hanged off from four thin nylon strings attached to the plate at its corners. This setup minimizes the energy dissipation during vibration. The free-free boundary condition is selected in this work because of the difficulties concerned with constructing rigid simple supports inducing no energy dissipation. The tests are performed according to Brüel & Kjær (B&K) modal testing method [31] and the setup is shown in Fig. 10. An accelerometer of 2.4 gram is attached to the center of the sandwich plate. The sandwich plate is excited by an impact hammer force applied close to the accelerometer. The

Table 1 – Constant parameters in Eqs. (37) and (38).

i	τ_i	E_i	G_i	i	τ_i	E_i	G_i
1	1.00E−11	0.00E+00	0.00E+00	11	1.97E−02	7.77E+05	3.85E+05
2	8.50E−11	0.00E+00	0.00E+00	12	1.67E−01	1.65E+06	7.76E+05
3	7.23E−10	3.25E+06	1.60E+06	13	1.42E+00	1.30E+06	6.20E+05
4	6.14E−09	3.60E+06	1.71E+06	14	1.21E+01	2.62E+06	1.24E+06
5	5.22E−08	3.61E+06	1.74E+06	15	1.03E+02	2.79E+06	1.31E+06
6	4.44E−07	2.75E+06	1.35E+06	16	8.72E+04	1.99E+06	9.10E+05
7	3.77E−06	1.98E+06	9.50E+05	17	Infinity	1.06E+07	4.85E+06
8	3.21E−05	1.38E+06	6.90E+05				
9	2.72E−04	3.48E+06	1.61E+06				
10	2.32E−03	1.34E+06	6.45E+05				

Table 2 – Stiffness properties of a unidirectional carbon/epoxy ply.

Property	E_1(GPa)	E_2(GPa)	G_{12}(GPa)	G_{23}(GPa)	υ_{12}	υ_{23}	ρ(kg/m^3)
Carbon/epoxy (T600)	96	12	6	3.5	0.3	0.714	1500

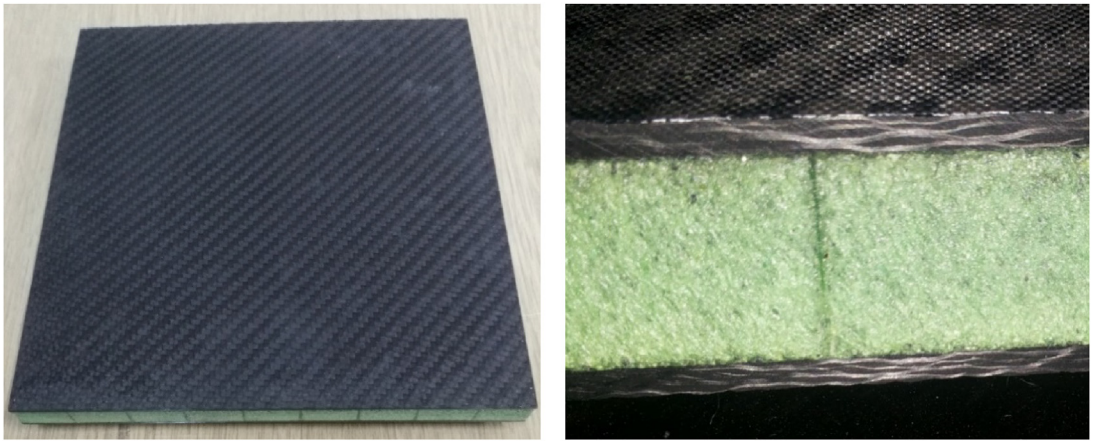

Fig. 9 – Composite sandwich plate made through vacuum infusion process.

Fig. 10 – Experimental setup for modal testing.

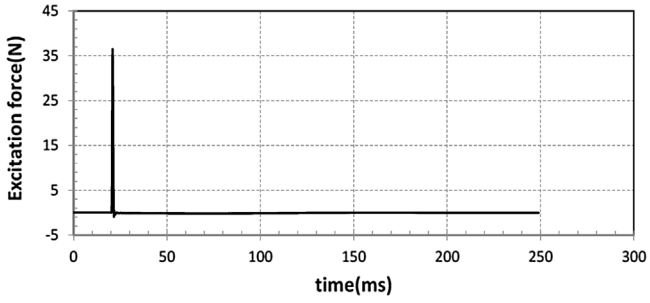

Fig. 11 – Excitation force versus time.

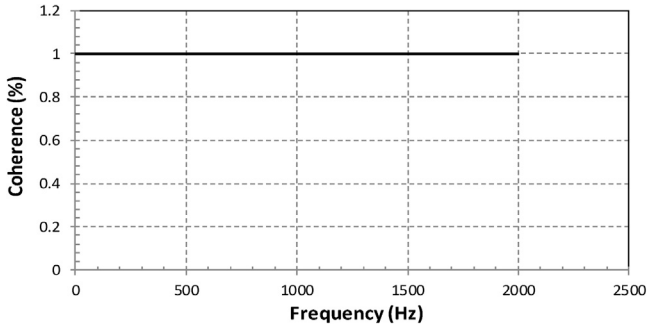

Fig. 12 – Coherence graph.

hammer force is measured by an internal sensor embedded in the hammer which is plotted versus time in Fig. 11.

The output response of the plate is measured by the accelerometer. A good impact produces a vibration response which is perfectly correlated with the impact. Such a good impact is conventionally indicated by a coherence graph that must be near to unity over the entire frequency range. A sample coherence graph for our tests is shown in Fig. 12 presenting the relevance of the hammer excitations applied here. Two type of modal tests are performed on the sandwich plate in this work, the first one in the air and the second in contact with bounded water. In the wet modal test only one side of the sandwich plate is in contact with water. A water tank of $500 \times 500 \times 1000$ mm is used for the wet modal test which is big enough to avoid the reflection of the waves [32] and [33].

5. Finite element analysis

Since the analytical exact solution developed in this work for simply supported sandwich plate is not applicable to the free-free plate, and on the other hand the construction of really rigid simple supports is not practical, the finite element method (FEM) is used as an intermediary between the experimental and analytical methods [34]. For this purpose, the two cases of the sandwich plate with simply supported as well as free-free sides are numerically analyzed by the finite element method to obtain both the dry and wet natural frequencies. The faces and the core of the sandwich plate are modeled by using brick elements. The mechanical properties of the viscoelastic foam and the orthotropic composite presented in Tables 1 and 2 are used as input to the modeling.

6. Results and discussion

In this section, the results of the present analytical method, modal testing, and the FEM are compared. The effects of the foam behavior and thickness, fiber orientation, plate dimension ratio, and fluid density on the natural frequency are examined and discussed.

6.1. *Experimental and finite element results and discussion*

From the plate midpoint acceleration data collected by the accelerometer, and the excitation force data, the real part and the absolute value of the frequency response function (FRF) are calculated and plotted versus frequency for both dry and wet plates as in Figs. 13 and 14, respectively. A comparison of the FRF absolute values for the dry and wet sandwich plates is shown in Fig. 15. The shapes of the frequency response function versus frequency graphs for the dry and wet sandwich plates are similar but shifted along the frequency axis with a factor of about 2 for frequency.

The natural frequencies of the sandwich plate are extracted from FRF graphs for the dry and wet conditions as presented in Table 3. It is noted that the natural frequencies are at the peak values of the absolute FRF graph if and only if there is a corresponding sudden change in the real part FRF graph. As shown in Table 3, the experimentally determined natural frequencies of the dry plate are about twice of those for the wet plate. This is attributed to the effect of the added mass of water contacting the sandwich plate.

The results of the FEM modal analysis for the mode shapes of the dry and wet sandwich plates with free-free and simply supported boundary conditions are shown in Figs. 16 and 17, respectively. Table 4 presents the natural frequencies of the dry and wet sandwich plates for the first three modes of vibration. As observed for the experimental results, the natural frequencies of the dry plate are about twice of those for the wet plate. On the other hand, the natural frequencies of the simply supported plate are always higher than those for the free-free plate, but their difference for the dry plate is more than that for the wet plate. Although there is a significant difference between the natural frequencies of the dry and wet plates, the mode shapes are quite similar for similar boundary conditions. It is concluded that the water added mass does not affect the mode shapes of the vibration.

A graphical comparison of the natural frequencies in Tables 3 and 4 for the experimental and free-free FEM model is shown in Fig. 18. It is observed that the experimental natural frequencies are higher than the numerical ones, not only for the dry but also for the wet plate. However, the frequency difference for the wet plate is less than that for the dry plate, 10–13% difference respectively. This is a reasonable difference between the FEM results and the experimental vibration measurements which are very sensitive to the boundary conditions. The creation of the real free-free boundary

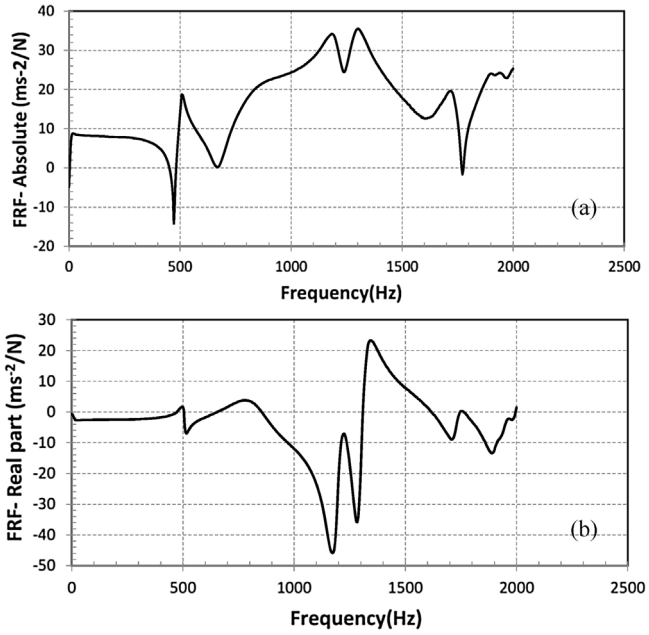

Fig. 13 – (a) Absolute value of FRF and (b) phase angle for dry sandwich plate.

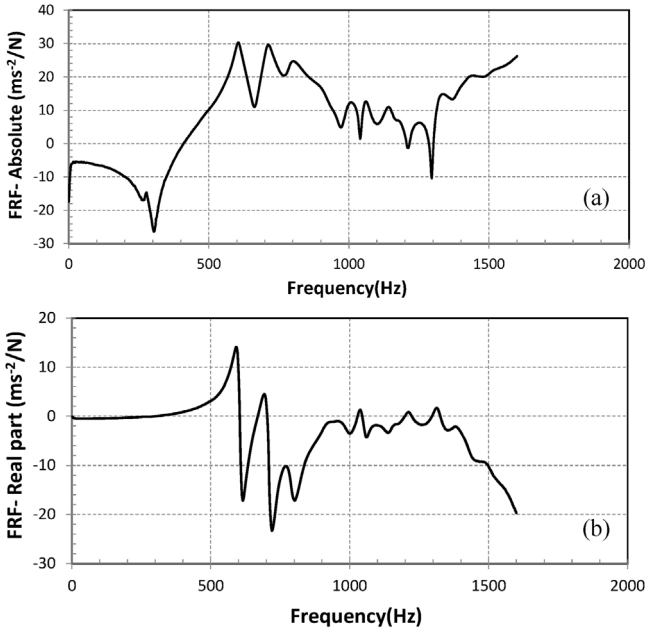

Fig. 14 – (a) Absolute value of FRF and (b) phase angle for wet sandwich plate.

condition for the plate is quite difficult in practice, and of course the results concern a reasonable error when using nylon strings.

6.2. *Analytical method results and discussion*

The analytical method of Navier's solution in this work is presented for simply supported sandwich plate and therefore its results are only compared with the FEM results as the

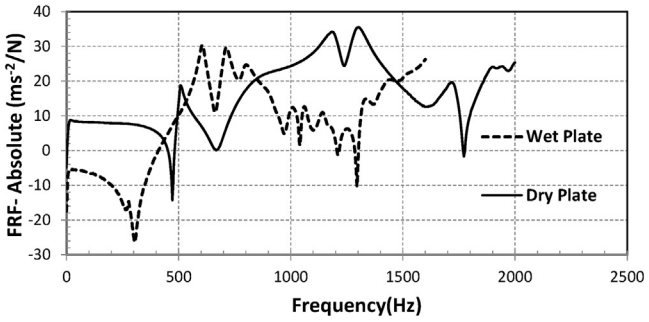

Fig. 15 – The absolute value of FRF for dry and wet plates together.

Table 3 – Experimental results for natural frequency of dry and wet sandwich free-free plates.

Mode number	Natural frequency (Hz)	
	Dry sandwich plate	Wet sandwich plate
1st mode	1200.1290	595.22
2nd mode	1305.0140	711.21
3rd mode	1736.7230	800.2941

intermediary explained in the previous section. The natural frequencies are analytically calculated for the dry and wet sandwich plates with different foam core behaviors, thicknesses, fiber orientations, plate dimension ratios, and fluid densities. The analytical and numerical first mode natural frequencies of the dry and wet plates are compared in the graphs of Fig. 19 for different plate dimension ratios, *c*/*d* in Fig. 1. It is observed that both of the analytical and numerical natural frequencies decrease with the increase of the plate dimension ratio which is due to the decrease of the flexural stiffness of the plate, see Fig. 19(a). Also, the ratio of the natural frequencies for the dry and wet plates slightly increases with the plate dimension ratio, see Fig. 19(b). This observation is attributed to the increase of the added mass effect on the plate having higher dimension ratios.

More importantly in Fig. 19(a), the analytical fundamental mode natural frequencies for both dry and wet plates are somewhat higher than the numerical ones. This difference is attributed to the approximation made in Eq. (13) by replacing the two integrals by the storage and loss modulus in the analytical method. Although this approximation has been necessary for our analytical solution, it slightly decreases the damping of the foam material and thus increases the analytical natural frequencies. Such an approximation is not necessary in the numerical FEM calculations where the relaxation functions of the foam are used directly.

One of the main capabilities of the present analytical closed form solution is the study of the influence of the viscoelastic against elastic behavior of the foam core on the natural frequencies of the sandwich plate. Two different mechanical behaviors are assumed for the foam core, the viscoelastic behavior as done above and an elastic behavior with constant Young's and shear moduli extracted from Figs. 6 and 7 at frequencies around the sandwich plate natural frequency. The

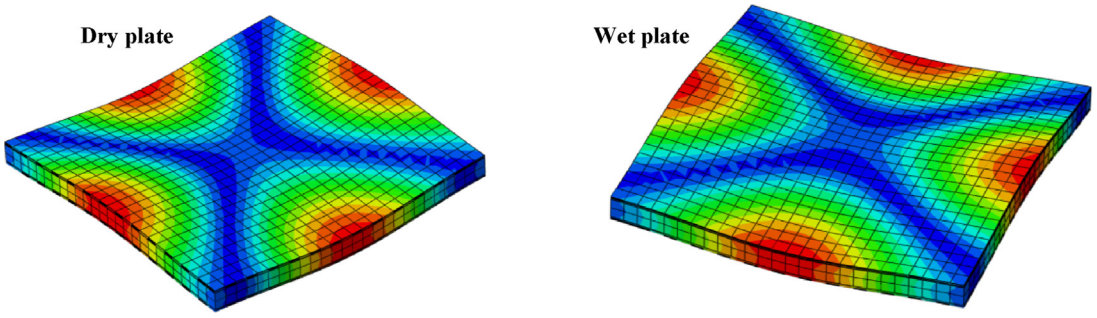

Fig. 16 – Mode shapes of the free-free dry and wet sandwich plates.

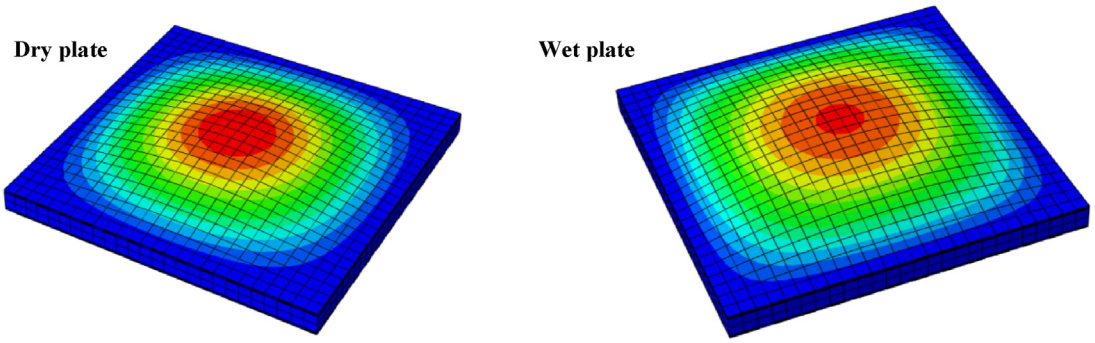

Fig. 17 – Mode shapes of the simply supported dry and wet sandwich plates.

Table 4 – FEM results for natural frequencies of the dry and wet sandwich plates.

Mode number	Natural frequency (Hz)	
	Dry sandwich plate Simply supported free-free	Wet sandwich plate Simply supported free-free
1st mode	1677.5 1039.9	839.4 532.5
2nd mode	2412.0 1188.2	994.7 654.6
3rd mode	2425.0 1504.8	996.2 724.7

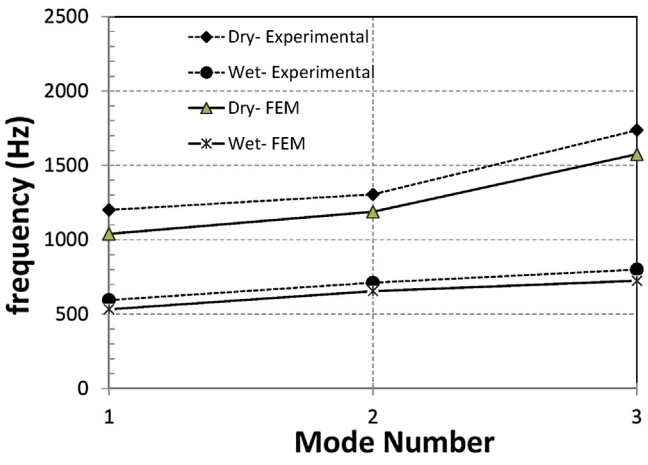

Fig. 18 – Comparison of experimental and FEM results for the first three modes of dry and wet sandwich plates.

results for the fundamental mode natural frequency of the dry and wet plates are summarized in Fig. 20. The decrease of the fundamental mode natural frequency with the presence of the viscoelastic foam core is observed for both dry and wet plates, however this effect is less prominent for the wet sandwich plate with respect to the dry one.

An alternative method to understand the significance of the viscoelastic core is presented in this work by studying the effect of the thickness of the foam core. The analytical solution is repeated for a series of sandwich plates consisting of identical face laminates but different core thicknesses from 5 up to 150 mm, see Fig. 21. It is observed that the fundamental mode natural frequency of the sandwich plate increases with the core thickness from 5 up to 70 mm where it starts to decrease. The increase of the fundamental mode natural frequency in the first part of the graph is attributed to the increase of the flexural stiffness of the sandwich plate which overrules the increase of the viscoelastic material. It is evident that above 70 mm thickness, the damping effect of the

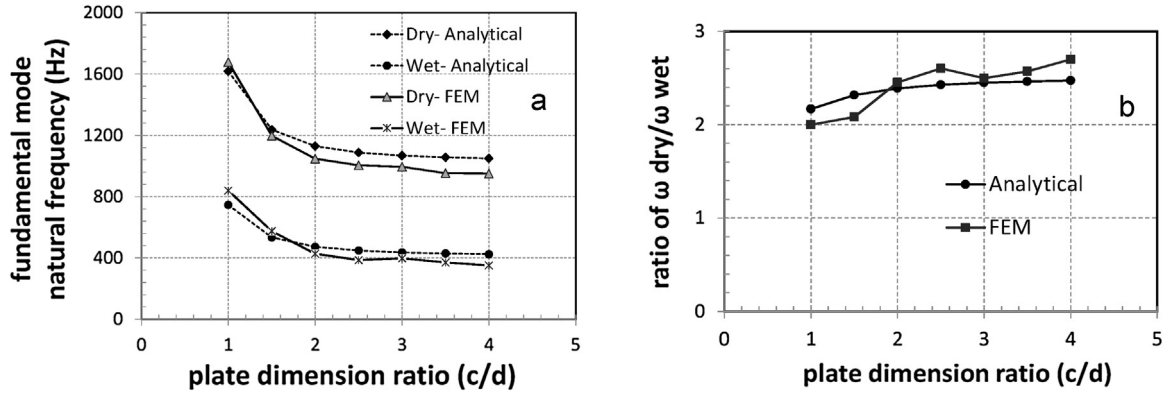

Fig. 19 – Comparison of analytical and FEM results for the fundamental mode natural frequency of dry and wet sandwich plates.

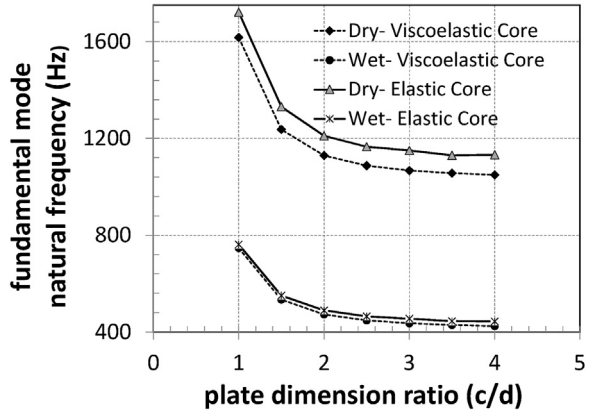

Fig. 20 – Analytical solution for the influence of the elastic and viscoelastic foam behaviors.

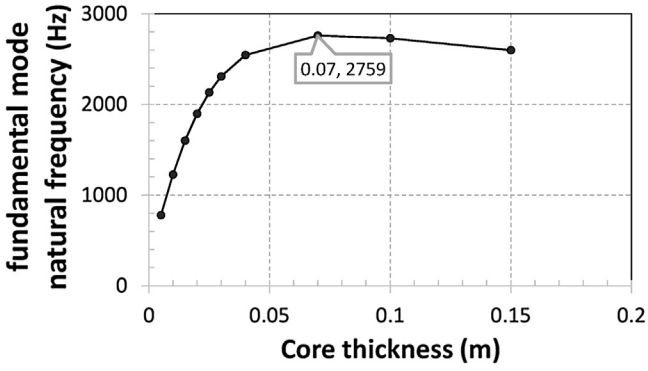

Fig. 21 – Variation of fundamental mode natural frequency versus core thickness.

Table 5 – Fundamental mode natural frequency of the sandwich plate (c/h = 13.4).

Plate dimension ratio c/d	Fundamental mode natural frequency (Hz)					
h_c/h	0.77	0.83	0.85	0.87	0.92	0.98
1	1616.9	1615.2	1607	1592.5	1506.5	1174.8
2	3781.2	3767.3	3748.4	3717.8	3543.7	2859.4
4	9561.4	9499.5	9455.2	9391.8	9073.3	7863.9

viscoelastic core overrules the increase of the plate flexural stiffness. When the total thickness of the sandwich plate h is fixed and the ratio of the core thickness h_c to the total thickness is increased, the analytical solution shows the decrease of the fundamental mode natural frequency, see Table 5. This is of course due to the decrease of the face thickness and thus the decrease of the sandwich plate stiffness.

The first five mode natural frequencies of the dry and wet sandwich plates obtained by the FEM method are shown in Fig. 22 for the free-free as well as simply supported conditions. It is observed that the influence of the water added mass is changing not only for different modes of vibration but also for different boundary conditions. The reason for the change of the added mass is the change of the shape of the plate vibrating in the water, and thus the amount of water that is moved by the plate at different modes and boundary conditions. Nevertheless, Fig. 22 shows that for both free-free and simply supported sandwich plates the changes of the natural frequencies from dry to wet condition remain within 50–70%, and it approaches to the same value of about 58% at higher modes of vibration.

As a continuation to the above discussion on the effect of the fluid, the fluid density is increased in the analytical method to obtain its effect on the fundamental mode natural frequency of the sandwich plate. Fig. 23 shows the decrease of the fundamental mode natural frequency with the fluid

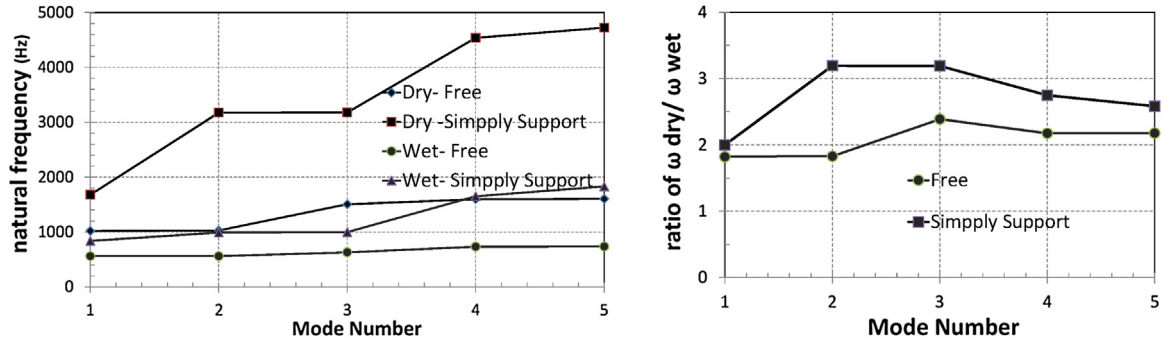

Fig. 22 – Effect of water in different modes of vibration and boundary conditions.

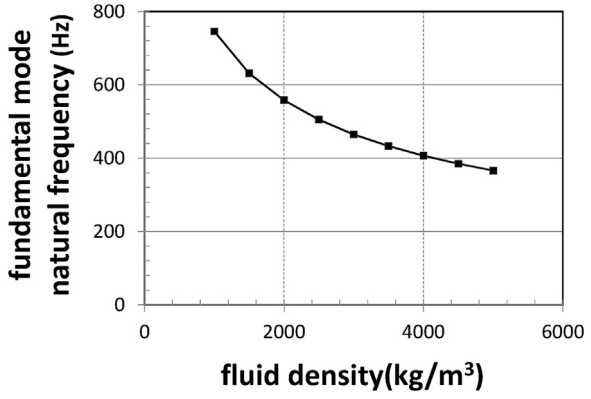

Fig. 23 – Effect of fluid density on fundamental mode natural frequency.

density. Also, the rate of decrease of the natural frequency is higher for the interval of low densities. This implies the lower effect of the fluid added mass at relatively high fluid densities.

7. Conclusions

In this study, the free vibration of a composite sandwich plate with a viscoelastic core in contact with bounded water is investigated both theoretically and experimentally for the first time. The kinetic and potential energy for the first-order shear-deformation sandwich plate with the kinetic energy of the bounded water are obtained and used in Hamilton's principle. The effect of water is therefore appeared as an added mass in the mass matrix. For the simply supported sandwich plate, the exact Navier's solution is used to construct the eigenvalue problem. In the experimental part of this work, eight layers of a thick woven carbon fabric as the face laminates and a marine PVC foam as the core material are applied in a vacuum infusion process to make a sandwich plate. Free-free boundary conditions are arranged for the sandwich plate in a hammer-accelerometer modal testing. FEM analysis is also used as an intermediary to verify the present analytical results. The conclusions may be summarized as below:

- The main novelty of the present study is the development of a closed form solution for the natural frequencies of a viscoelastic core sandwich plate at dry and wet conditions.
- The shapes of the graphs for the frequency response function vs frequency for the dry and wet sandwich plates are similar but shifted along the frequency axis with a factor of about 2 for frequency.
- It is experimentally found and analytically approved that the natural frequencies for the wet sandwich plate are about 50–70% of those for the dry sandwich plate. This demonstrates the validity of the analytical results.
- The decrease of the fundamental mode natural frequency with the presence of the viscoelastic foam core is more prominent for the dry sandwich plate with respect to the wet one already damped by water.
- The increase of the foam thickness has two different effects on the natural frequencies of the plate which are due to the opposite phenomena of increasing the stiffness as well as the damping of the plate.
- The effect of the added mass on the fundamental mode natural frequency of the sandwich plate decreases with the increase of the plate dimension ratio.
- The mode shape of the plate and its boundary condition affect the amount of the fluid moved by the plate and thus the value of the fluid added mass.

Appendix A. The force and moment resultants acting on the cross-section of the laminate.

$$
\begin{aligned}
N_x &= A_{11}\epsilon_{x0} + B_{11}K_x + A_{12}\epsilon_{y0} + B_{12}k_y + A_{13}\varphi_y + A_{14}\varphi_x + A_{15}\epsilon_{xy0} + B_{15}k_{xy}\\
N_y &= A_{21}\epsilon_{x0} + B_{21}K_x + A_{22}\epsilon_{y0} + B_{22}k_y + A_{23}\varphi_y + A_{24}\varphi_x + A_{25}\epsilon_{xy0} + B_{25}k_{xy}\\
N_{xy} &= A_{51}\epsilon_{x0} + B_{51}k_x + A_{52}\epsilon_{y0} + B_{52}k_y + A_{53}\varphi_y + A_{54}\varphi_x + A_{55}\epsilon_{xy0} + B_{55}k_{xy}\\
Q_y &= A_{31}\epsilon_{x0} + B_{31}k_x + A_{32}\epsilon_{y0} + B_{32}k_y + A_{33}\varphi_y + A_{34}\varphi_x + A_{35}\epsilon_{xy0} + B_{35}k_{xy}\\
Q_x &= A_{41}\epsilon_{x0} + B_{41}k_x + A_{42}\epsilon_{y0} + B_{42}k_y + A_{43}\varphi_y + A_{44}\varphi_x + A_{45}\epsilon_{xy0} + B_{35}k_{xy}\\
M_x &= B_{11}\epsilon_{x0} + D_{11}k_x + B_{12}\epsilon_{y0} + D_{12}k_y + B_{13}\varphi_y + B_{14}\varphi_x + B_{15}\epsilon_{xy0} + D_{15}k_{xy}\\
M_y &= B_{21}\epsilon_{x0} + D_{21}k_x + B_{22}\epsilon_{y0} + D_{22}k_y + B_{23}\varphi_y + B_{24}\varphi_x + B_{25}\epsilon_{xy0} + D_{25}k_{xy}\\
M_{xy} &= B_{51}\epsilon_{x0} + D_{51}kx + B_{25}\epsilon_{y0} + D_{52}k_y + B_{53}\varphi_y + B_{54}\varphi_x + B_{55}\epsilon_{xy0} + D_{55}k_{xy}
\end{aligned}
\tag{A.1}
$$

Appendix B. Five differential equations for displacement components and rotation functions.

$$
\begin{aligned}
&\partial u_0 : A_{11}\frac{\partial^2 u_0}{\partial x^2} + B_{11}\frac{\partial^2 \theta_x}{\partial x^2} + A_{12}\frac{\partial^2 v_0}{\partial x \partial y} + B_{12}\frac{\partial^2 \theta_y}{\partial x \partial y} + A_{13}\left(\frac{\partial^2 w_0}{\partial y \partial x} + \frac{\partial \theta_y}{\partial x}\right) +\\
&A_{14}\left(\frac{\partial^2 w_0}{\partial x^2} + \frac{\partial \theta_x}{\partial x}\right) + A_{15}\left(\frac{\partial^2 u_0}{\partial y \partial x} + \frac{\partial^2 v_0}{\partial x^2}\right) + B_{15}\left(\frac{\partial^2 \theta_x}{\partial y \partial x} + \frac{\partial^2 \theta_y}{\partial x^2}\right) +\\
&A_{51}\frac{\partial^2 u_0}{\partial x \partial y} + B_{51}\frac{\partial^2 \theta_x}{\partial x \partial y} + A_{52}\frac{\partial v_0^2}{\partial y^2} + B_{52}\frac{\partial^2 \theta_y}{\partial y^2} + A_{53}\left(\frac{\partial^2 w_0}{\partial y^2} + \frac{\partial \theta_y}{\partial y}\right) + A_{54}\left(\frac{\partial^2 w_0}{\partial x \partial y} + \frac{\partial \theta_x}{\partial y}\right) +\\
&A_{55}\left(\frac{\partial^2 u_0}{\partial y^2} + \frac{\partial^2 v_0}{\partial y \partial x}\right) + B_{55}\left(\frac{\partial^2 \theta_x}{\partial y^2} + \frac{\partial^2 \theta_y}{\partial x \partial y}\right) = I_1\omega^2 u + I_2\omega^2\theta_x
\end{aligned}
\tag{B.1}
$$

$$
\begin{aligned}
&\partial v_0 : A_{21}\frac{\partial^2 u_0}{\partial x \partial y} + B_{21}\frac{\partial^2 \theta_x}{\partial x \partial y} + A_{22}\frac{\partial^2 v_0}{\partial y^2} + B_{22}\frac{\partial^2 \theta_y}{\partial y^2} + A_{23}\left(\frac{\partial^2 w_0}{\partial y^2} + \frac{\partial \theta_y}{\partial y}\right) + A_{24}\left(\frac{\partial^2 w_0}{\partial x \partial y} + \frac{\partial \theta_x}{\partial y}\right) +\\
&A_{25}\left(\frac{\partial^2 u_0}{\partial y^2} + \frac{\partial^2 v_0}{\partial x \partial y}\right) + B_{25}\left(\frac{\partial^2 \theta_x}{\partial y^2} + \frac{\partial^2 \theta_y}{\partial x \partial y}\right) +\\
&A_{51}\frac{\partial^2 u}{\partial x^2} + B_{51}\frac{\partial^2 \theta_x}{\partial x^2} + A_{52}\frac{\partial^2 v_0}{\partial x \partial y} + B_{52}\frac{\partial^2 \theta_y}{\partial x \partial y} + A_{53}\left(\frac{\partial^2 w_0}{\partial x \partial y} + \frac{\partial \theta_y}{\partial x}\right) + A_{54}\left(\frac{\partial^2 w_0}{\partial x^2} + \frac{\partial \theta_x}{\partial x}\right) +\\
&A_{55}\left(\frac{\partial^2 u_0}{\partial x \partial y} + \frac{\partial^2 v_0}{\partial x^2}\right) + B_{55}\left(\frac{\partial^2 \theta_x}{\partial x \partial y} + \frac{\partial^2 \theta_y}{\partial x^2}\right) = I_1\omega^2 v + I_2\omega^2\theta_y
\end{aligned}
\tag{B.2}
$$

$$
\begin{aligned}
&\partial w_0 : A_{41}\frac{\partial^2 u_0}{\partial x^2} + B_{41}\frac{\partial^2 \theta_x}{\partial x^2} + A_{42}\frac{\partial^2 v_0}{\partial x \partial y} + B_{42}\frac{\partial^2 \theta_y}{\partial x \partial y} + A_{43}\left(\frac{\partial^2 w_0}{\partial x \partial y} + \frac{\partial \theta y}{\partial x}\right) + A_{44}\left(\frac{\partial^2 w_0}{\partial x^2} + \frac{\partial \theta_x}{\partial x}\right)\\
&+A_{45}\left(\frac{\partial^2 u_0}{\partial x \partial y} + \frac{\partial^2 v_0}{\partial x^2}\right) + B_{45}\left(\frac{\partial^2 \theta_x}{\partial x \partial y} + \frac{\partial^2 \theta_y}{\partial x^2}\right) + A_{31}\frac{\partial^2 u_0}{\partial x \partial y} + B_{31}\frac{\partial^2 \theta_x}{\partial x \partial y} + A_{32}\frac{\partial^2 v_0}{\partial y^2} + B_{32}\frac{\partial^2 \theta_y}{\partial y^2} +\\
&A_{33}\left(\frac{\partial^2 w_0}{\partial y^2} + \frac{\partial \theta_y}{\partial y}\right) + A_{34}\left(\frac{\partial^2 w_0}{\partial x \partial y} + \frac{\partial \theta_x}{\partial y}\right) + A_{35}\left(\frac{\partial^2 u_0}{\partial y^2} + \frac{\partial^2 v_0}{\partial x \partial y}\right) + B_{35}\left(\frac{\partial^2 \theta_x}{\partial y^2} + \frac{\partial^2 \theta_y}{\partial x \partial y}\right) =\\
&I_1\omega^2 w + (\omega^2 w \times m_a) = \omega^2 w(I_1 + m_a)
\end{aligned}
\tag{B.3}
$$

$$\begin{aligned}
&\delta\theta_x : B_{11}\frac{\partial^2 u_0}{\partial x^2}+D_{11}\frac{\partial^2 \theta_x}{\partial x^2}+B_{12}\frac{\partial^2 v_0}{\partial x\partial y}+D_{12}\frac{\partial^2 \theta_y}{\partial x\partial y}+B_{13}\left(\frac{\partial^2 w_0}{\partial x\partial y}+\frac{\partial \theta_y}{\partial x}\right)+\\
&B_{14}\left(\frac{\partial^2 w_0}{\partial x^2}+\frac{\partial \theta_x}{\partial x}\right)+B_{15}\left(\frac{\partial^2 u_0}{\partial x\partial y}+\frac{\partial^2 v_0}{\partial x^2}\right)+D_{15}\left(\frac{\partial^2 \theta_x}{\partial x\partial y}+\frac{\partial^2 \theta_y}{\partial x^2}\right)+\\
&B_{51}\frac{\partial^2 u_0}{\partial x\partial y}+D_{51}\frac{\partial^2 \theta_x}{\partial x\partial y}+B_{52}\frac{\partial^2 v_0}{\partial y^2}+D_{52}\frac{\partial^2 \theta_y}{\partial y^2}+B_{53}\left(\frac{\partial^2 w_0}{\partial y^2}+\frac{\partial \theta_y}{\partial y}\right)+B_{54}\left(\frac{\partial^2 w_0}{\partial x\partial y}+\frac{\partial \theta_x}{\partial y}\right)+\\
&B_{55}\left(\frac{\partial^2 u_0}{\partial y^2}+\frac{\partial^2 v_0}{\partial x\partial y}\right)+D_{55}\left(\frac{\partial^2 \theta_x}{\partial y^2}+\frac{\partial^2 \theta_y}{\partial x\partial y}\right)+\\
&\kappa_x^2(A_{41}\frac{\partial u_0}{\partial x}+B_{41}\frac{\partial \theta_x}{\partial x}+A_{42}\frac{\partial v_0}{\partial y}+A_{43}\left(\frac{\partial w_0}{\partial y}+\theta_y\right)+A_{44}\left(\frac{\partial w_0}{\partial x}+\theta_x\right)+A_{45}\left(\frac{\partial u_0}{\partial y}+\frac{\partial v_0}{\partial x}\right)\\
&+B_{35}\left(\frac{\partial \theta_x}{\partial y}+\frac{\partial \theta_y}{\partial x}\right))=I_2\omega^2 u+I_3\omega^2\theta
\end{aligned} \tag{B.4}$$

$$\begin{aligned}
&\delta\theta_y : B_{21}\frac{\partial^2 u_0}{\partial x\partial y}+D_{21}\frac{\partial^2 \theta_x}{\partial x\partial y}+B_{22}\frac{\partial^2 v_0}{\partial y^2}+D_{22}\frac{\partial^2 \theta_y}{\partial y^2}+B_{23}\left(\frac{\partial^2 w_0}{\partial y^2}+\frac{\partial \theta_y}{\partial y}\right)+\\
&B_{24}\left(\frac{\partial^2 w_0}{\partial x\partial y}+\frac{\partial \theta_x}{\partial y}\right)+B_{25}\left(\frac{\partial^2 u_0}{\partial y}+\frac{\partial^2 v_0}{\partial x\partial y}\right)+D_{25}\left(\frac{\partial^2 \theta_x}{\partial y^2}+\frac{\partial^2 \theta_y}{\partial x\partial y}\right)+\\
&B_{51}\frac{\partial^2 u_0}{\partial x^2}+D_{51}\frac{\partial^2 \theta_x}{\partial x^2}+B_{52}\frac{\partial^2 v_0}{\partial x\partial y}+D_{52}\frac{\partial^2 \theta_y}{\partial x\partial y}+B_{53}\left(\frac{\partial^2 w_0}{\partial x\partial y}+\frac{\partial \theta_y}{\partial x}\right)+B_{54}\left(\frac{\partial^2 w_0}{\partial x^2}+\frac{\partial \theta_x}{\partial x}\right)+\\
&B_{55}\left(\frac{\partial^2 u_0}{\partial x\partial y}+\frac{\partial^2 v_0}{\partial x^2}\right)+D_{55}\left(\frac{\partial^2 \theta_x}{\partial x\partial y}+\frac{\partial^2 \theta_y}{\partial x^2}\right)+\\
&\kappa_y^2(A_{31}\frac{\partial u_0}{\partial x}+B_{31}\frac{\partial \theta_x}{\partial x}+A_{32}\frac{\partial v_0}{\partial y}+B_{32}\frac{\partial^2 \theta_y}{\partial x\partial y}+A_{33}\left(\frac{\partial w_0}{\partial y}+\theta_y\right)+A_{34}\left(\frac{\partial w_0}{\partial x}+\theta_x\right)+\\
&A_{35}\left(\frac{\partial u_0}{\partial y}+\frac{\partial v_0}{\partial x}\right)+B_{35}\left(\frac{\partial \theta_x}{\partial y}+\frac{\partial \theta_y}{\partial x}\right))=I_2\omega^2 v+I_3\omega^2\theta
\end{aligned} \tag{B.5}$$

Appendix C. The elements of the mass matrix [M] and the real part of the stiffness matrix [K′].

$$[M]=\begin{bmatrix} m_{11}=I_1 & 0 & 0 & m_{14}=I_2 & 0\\ 0 & m_{21}=I_1 & 0 & 0 & m_{25}=I_2\\ 0 & 0 & m_{31}=(I_1+m_a) & 0 & 0\\ m_{41}=I_2 & 0 & 0 & m_{44}=I_3 & 0\\ 0 & m_{52}=I_2 & 0 & 0 & m_{55}=I_3 \end{bmatrix} \tag{C.1}$$

$$\begin{aligned}
k'_{11}&=A_{11}\alpha^2+A_{15}\alpha\beta+A_{51}\alpha\beta+A_{55}\beta^2\\
k'_{12}&=A_{12}\alpha\beta+A_{15}\alpha^2+A_{52}\beta^2+A_{55}\alpha\beta\\
k'_{13}&=A_{13}\alpha\beta+A_{14}\alpha^2+A_{53}\beta^2+A_{54}\alpha\beta\\
k'_{14}&=B_{11}\alpha^2+A_{14}\alpha+B_{15}\alpha\beta+B_{51}\alpha\beta+A_{54}\beta+B_{55}\beta^2\\
k'_{15}&=B_{12}\alpha\beta+A_{13}\alpha+B_{15}\alpha^2+B_{52}\beta^2+A_{53}\beta+B_{55}\alpha\beta
\end{aligned} \tag{C.2}$$

$$\begin{aligned}
k'_{21}&=A_{21}\alpha\beta+A_{25}\beta^2+A_{51}\alpha^2+A_{55}\alpha\beta\\
k'_{22}&=A_{22}\beta^2+A_{25}\alpha\beta+A_{52}\beta\alpha+A_{55}\alpha^2\\
k'_{23}&=A_{23}\beta^2+A_{24}\alpha\beta+A_{53}\alpha\beta+A_{54}\alpha^2\\
k'_{24}&=B_{21}\alpha\beta+A_{24}\beta+B_{25}\beta^2+B_{51}\alpha^2+A_{54}\alpha+B_{55}\alpha\beta\\
k'_{25}&=B_{22}\beta^2+A_{23}\beta+B_{25}\alpha\beta+B_{52}\alpha\beta+A_{53}\alpha+B_{55}\alpha^2
\end{aligned} \tag{C.3}$$

$$\begin{aligned}
k'_{31}&=A_{41}\alpha^2+A_{45}\alpha\beta+A_{31}\alpha\beta+A_{35}\beta^2\\
k'_{32}&=A_{42}\alpha\beta+A_{45}\alpha^2+A_{32}\beta^2+A_{35}\alpha\beta\\
k'_{33}&=A_{43}\alpha\beta+A_{44}\alpha^2+A_{33}\beta^2+A_{34}\alpha\beta\\
k'_{34}&=B_{41}\alpha^2+A_{44}\alpha+B_{45}\alpha\beta+B_{31}\alpha\beta+A_{34}\beta+B_{35}\alpha\beta\\
k'_{35}&=B_{42}\alpha\beta+A_{43}\alpha+B_{45}\alpha^2+B_{32}\beta^2+A_{33}\beta+B_{35}\alpha\beta
\end{aligned} \tag{C.4}$$

$$
\begin{aligned}
k'_{41} &= B_{11}\alpha^2 + B_{15}\alpha\beta + B_{51}\alpha\beta + B_{55}\beta + \kappa_x^2(A_{41}\alpha + A_{45}\beta)\\
k'_{42} &= B_{12}\alpha\beta + B_{15}\alpha^2 + B_{52}\beta^2 + B_5\alpha\beta + \kappa_x^2(A_{42}\beta + A_{45}\alpha)\\
k'_{43} &= B_{13}\alpha\beta + B_{14}\alpha^2 + B_{53}B^2 + B_{54}\alpha\beta + \kappa_x^2(A_{43}\beta + A_{44}\alpha)\\
k'_{44} &= D_{11}\alpha^2 + B_{14}\alpha + D_{15}\alpha\beta + D_{51}\alpha\beta + B_{54}\beta + D_{55}\beta^2 + \kappa_x^2(B_{41}\alpha + A_{44} + B_{45}\beta)\\
k'_{45} &= D_{12}\alpha\beta + B_{13}\alpha + D_{15}\alpha^2 + D_{52}\beta^2 + B_{53}\beta + D_{55}\alpha\beta + \kappa_x^2(A_{43} + \beta_{45}\alpha)
\end{aligned}
\tag{C.5}
$$

$$
\begin{aligned}
k'_{51} &= B_{21}\alpha\beta + B_{25}\beta^2 + B_{51}\alpha^2 + B_{55}\alpha\beta + \kappa_y^2(A_{31}\alpha + A_{35}\beta)\\
k'_{52} &= B_{22}\beta^2 + B_{25}\alpha\beta + B_{52}\alpha\beta + B_{55}\alpha^2 + \kappa_y^2(A_{32}\beta + A_{35}\alpha)\\
k'_{53} &= B_{23}\beta^2 + B_{24}\alpha\beta + B_{53}\alpha\beta + B_{54}\alpha^2 + \kappa_y^2(A_{33}\beta + A_{34}\alpha)\\
k'_{54} &= D_{21}\alpha\beta + B_{24}\beta + D_{25}\beta^2 + D_{51}\alpha^2 + D_{55}\alpha\beta + \kappa_y^2(B_{31}\alpha + A_{34} + B_{34}\beta)\\
k'_{55} &= D_{22}\beta^2 + B_{23}\beta + D_{25}\alpha\beta + D_{52}\alpha B + B_{53}\alpha + D_{55}\alpha^2 + \kappa_y^2(B_{32}\beta + A_{33} + B_{35}\alpha)
\end{aligned}
\tag{C.6}
$$

REFERENCES

[1] P. Cupiał, J. Nizioł, Vibration and damping analysis of a three-layered composite plate with a viscoelastic mid-layer, J. Sound Vib. 183 (1995) 99–114.

[2] T. Kant, K. Swaminathan, Analytical solutions for free vibration of laminated composite and sandwich plates based on a higher-order refined theory, Compos. Struct. 53 (2001) 73–85.

[3] H.-J. Wang, L.-W. Chen, Vibration and damping analysis of a three-layered composite annular plate with a viscoelastic mid-layer, Compos. Struct. 58 (2002) 563–570.

[4] T.-W. Kim, J.-H. Kim, Nonlinear vibration of viscoelastic laminated composite plates, Int. J. Solids Struct. 39 (2002) 2857–2870.

[5] Z.-D. Xu, H.-T. Zhao, A.-Q. Li, Optimal analysis and experimental study on structures with viscoelastic dampers, J. Sound Vib. 273 (2004) 607–618.

[6] Y.-R. Chen, L.-W. Chen, Vibration and stability of rotating polar orthotropic sandwich annular plates with a viscoelastic core layer, Compos. Struct. 78 (2007) 45–57.

[7] Ö. Civalek, Free vibration analysis of symmetrically laminated composite plates with first-order shear deformation theory (FSDT) by discrete singular convolution method, Finite Elem. Anal. Des. 44 (2008) 725–731.

[8] V. Birman, C.W. Bert, On the choice of shear correction factor in sandwich structures, J. Sandwich Struct. Mater. 4 (2002) 83–95.

[9] A. Bhar, S. Phoenix, S. Satsangi, Finite element analysis of laminated composite stiffened plates using FSDT and HSDT: a comparative perspective, Compos. Struct. 92 (2010) 312–321.

[10] H. Asadi, M. Souri, Q. Wang, A numerical study on flow-induced instabilities of supersonic FG-CNT reinforced composite flat panels in thermal environments, Compos. Struct. 171 (2017) 113–125.

[11] M.M. Keleshteri, H. Asadi, Q. Wang, Large amplitude vibration of FG-CNT reinforced composite annular plates with integrated piezoelectric layers on elastic foundation, Thin-Walled Struct. 120 (2017) 203–214.

[12] A. Assie, M. Eltaher, F. Mahmoud, Behavior of a viscoelastic composite plates under transient load, J. Mech. Sci. Technol. 25 (2011) 1129–1140.

[13] S. Mahmoudkhani, H. Haddadpour, H.M. Navazi, Free and forced random vibration analysis of sandwich plates with thick viscoelastic cores, J. Vib. Control 19 (2013) 2223–2240.

[14] M.R. Kramer, Z. Liu, Y.L. Young, Free vibration of cantilevered composite plates in air and in water, Compos. Struct. 95 (2013) 254–263.

[15] J. Yang, J. Xiong, L. Ma, B. Wang, G. Zhang, L. Wu, Vibration and damping characteristics of hybrid carbon fiber composite pyramidal truss sandwich panels with viscoelastic layers, Compos. Struct. 106 (2013) 570–580.

[16] K. Khorshid, S. Farhadi, Free vibration analysis of a laminated composite rectangular plate in contact with a bounded fluid, Compos. Struct. 104 (2013) 176–186.

[17] M. Mehri, H. Asadi, Q. Wang, On dynamic instability of a pressurized functionally graded carbon nanotube reinforced truncated conical shell subjected to yawed supersonic airflow, Compos. Struct. 153 (2016) 938–951.

[18] M.S. Kiasat, H.A. Zamani, M.M. Aghdam, On the transient response of viscoelastic beams and plates on viscoelastic medium, Int. J. Mech. Sci. 83 (2014) 133–145.

[19] M. Avcar, Effects of rotary inertia shear deformation and non-homogeneity on frequencies of beam, Struct. Eng. Mech. 55 (4) (2015) 871–884.

[20] C. Yang, G. Jin, X. Ye, Z. Liu, A modified Fourier–Ritz solution for vibration and damping analysis of sandwich plates with viscoelastic and functionally graded materials, Int. J. Mech. Sci. 106 (2016) 1–18.

[21] V. Kahya, M. Turan, Finite element model for vibration and buckling of functionally graded beams based on the first-order shear deformation theory, Compos. B: Eng. 109 (2017) 108–115.

[22] M. Rezaee Sangtabi, M.S. Kiasat, Long-term viscoelastic properties of an adhesive and molding compound, characterization and modeling, Polymer 116 (2017) 204–217.

[23] D.S. Cho, B.H. Kim, J.-H. Kim, N. Vladimir, T.M. Choi, Frequency response of rectangular plate structures in contact with fluid subjected to harmonic point excitation force, Thin-Walled Struct. 95 (2015) 276–286.

[24] K.R. Pradeep, B.N. Rao, S.M. Srinivasan, K. Balasubramaniam, S. Ahamed, Influence of core compressibility, flexibility and transverse shear effects on the response of sandwich structures, Am. J. Mech. Ind. Eng. 2 (2) (2017) 81–91.

[25] J. Zhang, G. Xu, F. Liu, J. Lian, X. Yan, Experimental investigation on the flow induced vibration of an equilateral triangle prism in water, Appl. Ocean Res. 61 (2016) 92–100.

[26] A.S. Sayyad, Y.M. Ghugal, On the free vibration analysis of laminated composite and sandwich plates: a review of recent literature with some numerical results, Compos. Struct. 129 (2015) 177–201.

[27] M.S. Kiasat, M. Rezaee Sangtabi, Effects of fiber bundle size and weave density on stiffness degradation and final failure of fabric laminates, Compos. Sci. Technol. 111 (2015) 23–31.

[28] J.D. Ferry, Viscoelastic Properties of Polymers, John Wiley & Sons, 1980.

[29] M.S. Kiasat, G. Zhang, L. Ernst, G. Wisse, Creep behavior of a molding compound and its effect on packaging process stresses, in: Electronic Components and Technology Conf, 2001, 931–938.

[30] C. Cooper, R. Young, M. Halsall, Investigation into the deformation of carbon nanotubes and their composites through the use of Raman spectroscopy, Compos. A: Appl. Sci. Manuf. 32 (2001) 401–411.

[31] K. Torabi, M. Shariati-Nia, M. Heidari-Rarani, Experimental and theoretical investigation on transverse vibration of delaminated cross-ply composite beams, Int. J. Mech. Sci. 115 (2016) 1–11.

[32] T. Brugo, R. Panciroli, G. Minak, Study of the dynamic behavior of plates immersed in a fluid, in: Experimental Mechanics Conf., 2012.

[33] S. Hosseini Hashemi, M. Karimi, H. Rokni, Natural frequencies of rectangular Mindlin plates coupled with stationary fluid, Appl. Math. Model. 36 (2012) 764–778.

[34] S.K. Lee, M.W. Kim, C.J. Park, M.J. Chol, G. Kim, J.-M. Cho, G. Kim, J.-M. Cho, C.-H. Choi, Effect of fiber orientation on acoustic and vibration response of a carbon fiber/epoxy composite plate: Natural vibration mode and sound radiation, Int. J. Mech. Sci. 117 (2016) 162–173.